Available online at www.sciencedirect.com

ScienceDirect

Procedia IUTAM 26 (2018) 194–203

Procedia IUTAM

www.elsevier.com/locate/procedia

IUTAM Symposium Wind Waves, 4–8 September 2017, London, UK

Quasi-linear approximation for description of turbulent boundary layer and wind wave growth

Yu. Troitskaya[a,b,d]*, O.Druzhinin[a,b], D.Sergeev[a,b], A.Kandaurov[a,b], O.Ermakova[a,b], W. t. Tsai[c]

[a]*Institute of Applied Physics, Nizhny Novgorod, 603950, Russia,*
[b]*Nizhny Novgorod State University, Nizhny Novgorod, 603022, Russia*
[c]*National Taiwan University/Department of Engineering Science and Ocean Engineering, Taipei, 10617, Taiwan*
[d]*Obukhov Institute of Atmospheric Physics, Moscow, 143039, Russia*

Abstract

This study describes an approximate quasi-linear model for the description of the turbulent boundary layer over steep surface waves. The model assumes that wave-induced disturbances of the atmospheric turbulent boundary layer could be reasonably described in a linear approximation with the momentum flux from wind to waves retained as the only nonlinear effect in the model. For the case of periodic long-crested waves, the model has been verified with a set of the original laboratory and numerical experiments. The laboratory experimental study of the airflow over the steep waves was performed by means of the PIV technique. The numerical study was performed with direct numerical simulation (DNS) of the turbulent airflow over waved surface at Re=15,000 for quasi-homogeneous waves, wave trains and parasitic capillaries riding on the crest of a steep waves. Examples are given of the application of the quasi-linear approximation to describe the turbulent boundary layer over waves with the continuous spectrum under the assumption of random phases of harmonics. In the latter case the quasi-linear model provides the growth rate of surface waves in the inertial interval of the surface wave spectrum proportional to w7/3 in agreement with predictions in [1].

Peer-review under responsibility of the scientific committee of the IUTAM Symposium Wind Waves.

Keywords: wind; turbulence; atmospheric boundary layer; wind waves; DNS

* Corresponding author Yu. Troitskaya. Tel.: +7-831-436-8297; fax: +0-000-000-0000 .
E-mail address: yuliya@hydro.appl.sci-nnov.ru

2210-9838
Peer-review under responsibility of the scientific committee of the IUTAM Symposium Wind Waves.
10.1016/j.piutam.2018.03.019

1. Introduction

Interaction of the wind flow with surface waves is one of the central questions in the wave modelling, because it defines the wind input to waves. In spite of significant progress in the topic there is a number of questions, the most essential of which is strong dispersion in wind input obtained in different experiments, which is about 300–500% [1-3]. It is one of possible sources of errors in forecasts of wind waves.

Measuring wind input is a quite tricky experimental problem. The energy flux from wind to waves is determined by surface stresses (pressure and tangential stresses) at the water surface, which should be measured at curved liquid surface, including areas below the wave crests. These measurements can be performed by a wave-following contact technique [4-6]. Measurements of airflow below crests of the waves can be performed by seeding the flow with small particles visualized with a strobe source of light and application of special photograph technique [7]. Kawai's experiments demonstrated occurrence of the airflow separation from the crests of steep waves in a set of instant images. The state-of-art method applicable for investigation the structure of airflow over waves is the particle image velocimetry (PIV) [9]. In this method, the flow is seeded with small particles illuminated by laser beam, which makes them visible on digital images. Applications of the PIV in [10-14] clearly demonstrated a complex turbulent airflow with pronounced flow separation from the crests of waves and reattachment at the windward face of the wave on the instantaneous patterns of the vector velocity fields.

It should be noted that the separation of wind flow from the crest of the surface wave is a non-stationary turbulent process with a characteristic scale that is small compared with the period of the wave. It can be expected that the processes of turbulent exchange between the ocean and the atmosphere and wind induced generation of waves, whose timescales greatly exceed the period of the wave, are caused by the wind flow fields averaged over the turbulent pulsations. The velocity fields averaged over turbulent pulsations are smooth and un-separated. It was confirmed by averaging over the statistical ensembles of realizations of instantaneous velocity fields obtained with use of the time-resolved PIV in [13] and individual instantaneous vector velocity fields retrieved from the planar PIV in [14]. It encourage us to use the quasi-linear approximation for description of coupling of surface waves with turbulent atmospheric boundary layer, where wave-induced air-flow disturbances are described in linear approximation.

2. Formulation of the quasi--linear model of turbulent wind over waved water surface

There exists two classes of quasi-linear models, which can be distinguished by the model of wind wave growth. The first class (e.g., [15, 16]) is based on the quasi-laminar model [16, 17] model of wind wave growth. The second class (e.g., [19, 20]) assumes that the wind wave growth is governed by the effect of eddy viscosity.

Visualization of the air flow over steep wind waves [13] clearly demonstrates that turbulent vortices are much faster than waves. Then a model based on RANS (Reynolds-Averaged Navier-Stokes) equations can be used to describe the turbulent air flow over waves. The model reads:

$$\frac{\partial \langle u_i \rangle}{\partial t} + \langle u_j \rangle \frac{\partial \langle u_i \rangle}{\partial x_j} + \frac{1}{\rho_a} \frac{\partial \langle p \rangle}{\partial x_i} = \frac{\partial \sigma_{ij}}{\partial x_j} \tag{1}$$

where the turbulence stress tensor is:

$$\sigma_{ij} = \langle u_i' u_j' \rangle = \nu \left(\frac{\partial \langle u_i \rangle}{\partial x_j} + \frac{\partial \langle u_j \rangle}{\partial x_i} \right) \tag{2}$$

Here, <...> denotes the averaging operation over ensemble of turbulent fluctuations, ν is the turbulent eddy viscosity coefficient, which is a self-similar function of the distance, z, from the air-water interface:

$$\nu = \nu_a f\left(\frac{z u_*}{\nu_a}\right), \tag{3}$$

where v_a is the air molecular viscosity, u_* is the friction velocity in the turbulent boundary layer. We used an empirical approximation for the function f obtained in [21].

$$\nu = \nu_a \left\{1 + \kappa \frac{u_* \eta \sqrt{\tau_{turb}/u_*^2}}{\nu_a}\left[1 - e^{-\frac{1}{L}\left(\frac{u_* \eta}{\nu_a}\right)^2 \left(\frac{\tau_{turb}}{u_*^2}\right)}\right]\right\} \tag{4}$$

In this expression, L is the scale of a viscous sub-layer, which depends on a flow regime. [21] suggested L=22.4 for the aerodynamically smooth surface that gives the roughness height of 0.11 ν_a / u_*. We consider the air-water interface in our approximate model as an aerodynamically smooth curved surface.

The boundary conditions at the air-water interface $z=\xi(x,y,t)$ are:

$$\frac{\partial \xi}{\partial t} + \langle u \rangle \frac{\partial \xi}{\partial x} + \langle v \rangle \frac{\partial \xi}{\partial y}\bigg|_{z=\xi(x,y,t)} = \langle w \rangle\big|_{z=\xi(x,y,t)} \tag{5}$$

$$\left\langle \vec{u}_\tau^{\,w} \right\rangle\big|_{z=\xi(x,y,t)} = \left\langle \vec{u}_\tau^{\,a} \right\rangle\big|_{z=\xi(x,y,t)}, \tag{6}$$

$\langle u \rangle$, $\langle v \rangle$, $\langle w \rangle$ are the averaged air velocity components aligned with the x-, y- and z- axes. To avoid strong geometrical nonlinearity we formulated RANS equations in the wave-following curvilinear coordinates.

The solution to the set of the Reynolds equations is searched as a sum of the mean flow and wave induced disturbances. Contrary to the turbulent vortices the wind interaction with waves is not parameterized, but described directly, within the approximate quasi-linear model, when the wave-induced disturbances of the air flow are considered within the linear approximation and the higher harmonics of perturbations are neglected. The only non-linear effect taken into account is the deformation of the mean flow velocity due to momentum flux to wave and the only nonlinear equation describes the momentum flux from wind to waves, which is completely determined by the three-dimensional surface wave spectrum (dependent on wave number, frequency and angle). The equations of the quasi-linear model used here are given in [22, 23]. The quasi-linear approach is applicable for small Reynolds numbers (see [24]). Although the Reynolds number Re_{eff} defined by the molecular viscosity is huge in turbulent flows, but the flow averaged over turbulent fluctuations described within the RANS equations is determined by the effective Reynolds number, which is defined by the eddy viscosity coefficient. Estimates in [13] show that $Re_{eff} \sim ka<1$, that confirms the quasi-linear approximation.

3. Verification of the quasi-linear model

Strong assumptions behind the quasi-linear approximation for disturbances induced by surface waves in the marine atmospheric boundary layer need to be verified on the base of laboratory physical and numerical experiments. In the physical experiment, turbulent airflow in a laboratory tank over mechanically generated periodic surface waves was studied with the use of the planar time-resolved PIV technique, based on high-speed video photography (see [13]). The data of these measurements were compared with the predictions of the quasi- linear model for the parameters of the waves (wavelength, celerity, steepness) and the air-flow (wind friction velocity and roughness height) retrieved from the experiment. The model reproduced not only the average velocity and stress profiles, but the parameters of the wave-induced velocity and pressure disturbances averaged over turbulent fluctuations. The latter can be retrieved directly from the RANS equations, since the time-resolved PIV gives the sequences of instant air flow velocity fields. In case of long-crested waves, the momentums of the air-flow velocity

fields are two-dimensional, and planar PIV is sufficient for retrieval average pressure field directly from the RANS – equations as follows:

$$\left(\frac{\langle p\rangle}{\rho_a}-\sigma_{33}\right)\Bigg|_{x_3-\xi(x_1,t)}^{H-\xi(x_1,t)}=-\int_{x_3-\xi(x_1,t)}^{H-\xi(x_1,t)}\left[\frac{\partial\langle v_3\rangle}{\partial t}+\frac{\partial}{\partial x_1}\left(\langle v_1\rangle\cdot\langle v_3\rangle-\sigma_{13}\right)\right]dx_3+$$
$$-\left[\langle v_3\rangle\left(\langle v_3\rangle-\left(\frac{\partial\xi(x_1,t)}{\partial t}+\langle v_1\rangle\frac{\partial\xi(x_1,t)}{\partial x_1}\right)\right)+\sigma_{13}\frac{\partial\xi(x_1,t)}{\partial x_1}\right]\Bigg|_{x_3-\xi(x_1,t)}^{H-\xi(x_1,t)} \tag{7}$$

Here H is the top boundary of the measuring domain.

3.1. Direct numerical simulation of turbulent boundary layer over waved water surface. Quasi-harmonic waves

The question why the simple quasi-linear approximation is applicable for description of the strongly nonlinear effect was studied within the direct numerical simulation (DNS) of the detailed structure and statistical characteristics of turbulent boundary layer over finite amplitude periodic surface wave [25]. These DNS modelled two-dimensional water waves with the wave slopes in the range ka=0-0.2 in the flow with the bulk Reynolds number Re = 15000. A number of wave age parameters in the range $c/u_* = 0 - 10$ where u_* is the friction velocity and c is the wave celerity were considered. The computational domain (periodic in the x- and y-directions) had the size $L_x = 6\lambda$, $L_y = 4\lambda$ and $L_z = \lambda$. The DNS code was solving fully three-dimensional Navier-Stokes equations in curvilinear coordinates in the frame of reference moving with the phase velocity of the wave. The flow was driven by the shear, which was created by the upper plane boundary moving horizontally in the x-direction with a prescribed bulk velocity.

Similarly to the physical experiment the instant realizations of the velocity field demonstrate flow separation at the crests of the waves, but the ensemble averaged velocity fields had typical structures similar to those existing in shear flows near critical levels, where the phase velocity of the disturbance coincides with the flow velocity [25]. Comparison with the calculations within the quasi-linear model showed, that the DNS runs supported the applicability of the quasi-linear model for description profiles of the mean wind velocity, the turbulent stress, amplitude and phase of the main harmonics of the wave-induced velocity components. This is confirmed by the close structures of the exact and approximate patterns of streamlines in the airflow above the waves with different steepness (Fig. 1).

The magnitude and phase of wave induced pressure fluctuations obtained within the quasi-linear model are also in a good agreement with the DNS data (see Fig. 2 (a), (b)). Fig. 2 (c) confirms, that the model reproduces the wind-wave interaction parameter as it was introduced by Miles (1957):

$$\beta=\frac{2}{(ka)^2\rho u_*^2}\frac{1}{\lambda}\int_0^{\lambda}\langle p\rangle\frac{d\xi}{dx}dx\,, \tag{8}$$

which determines the wind wave growth rate: $\mathrm{Im}\,\omega=\frac{1}{2}\frac{u_*^2}{c^2}\beta\frac{\rho_a}{\rho_w}\omega$. Notice the decrease of the wind-wave growth rate parameter β with the increase of the wave steepness (see Fig. 2 (c)).

The DNS results support applicability of the non-separating quasi-linear theory for description of average fields in the airflow over steep and even breaking waves, when the effect of separation is manifested in the instantaneous flow images and is explained by strong inhomogeneity of the separation zone in the transversal direction (along the wave front), shown in DNS. It appears that the vorticity is mostly concentrated in thread-like vortex structures, which have a horseshoe shape and resemble well-known λ-vortices extensively studied in the case of a "classical" boundary layer over a solid plane boundary [26]. The similar strongly inhomogeneous separation of the flow from the wave crests and the Kelvin cat-eyes patterns in the mean flow field were observed in DNS [27].

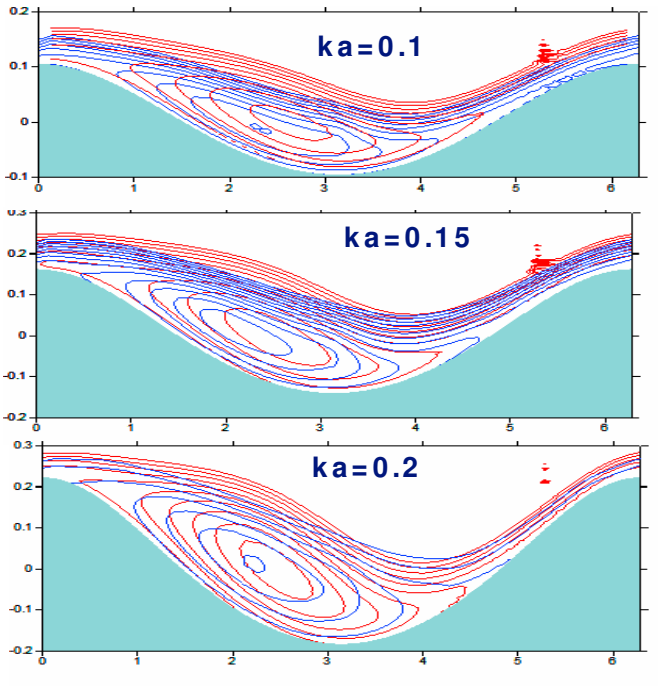

Fig.1. The streamline patters in the air flow over waves in the wave-following reference frame. The red lines - results of DNS, the blue lines – the quasi-linear model. Numbers at the curves are the wave steepness, $c/u_* \approx 1.6$.

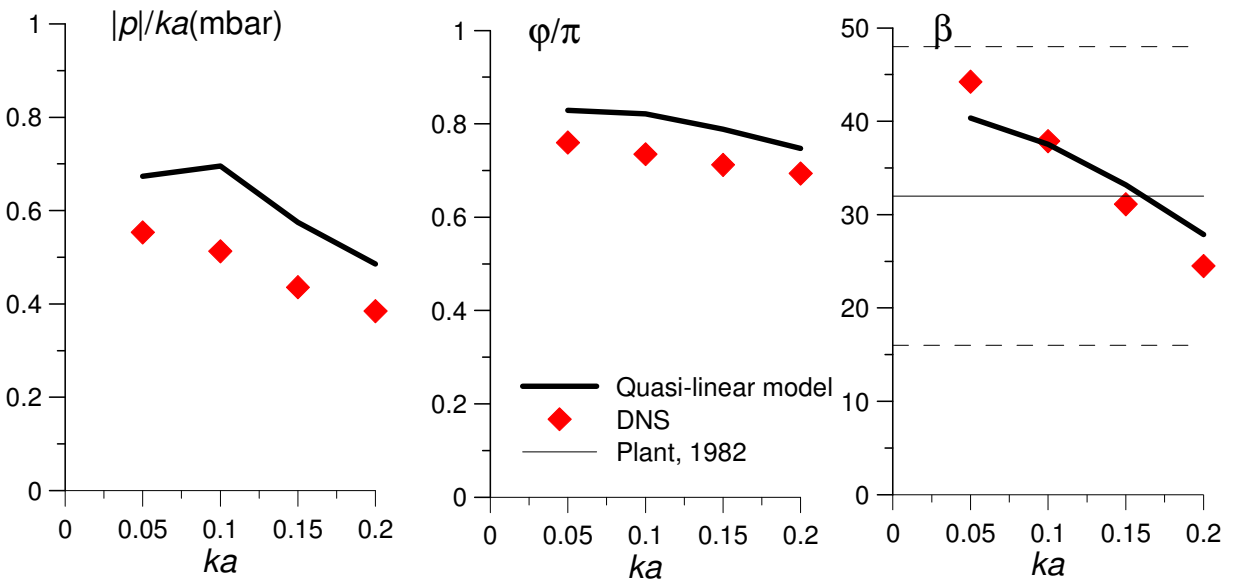

(a) (b) (c)

Fig.2. Comparing theory and DNS: magnitude (a) and phase shift (b) of the wave-induced pressure disturbances at the water surface, the Miles (1957) wind-wave interaction parameter β (c) via wave steepness. The bold line presents calculations within the quasi-linear model, symbols are the results of DNS.

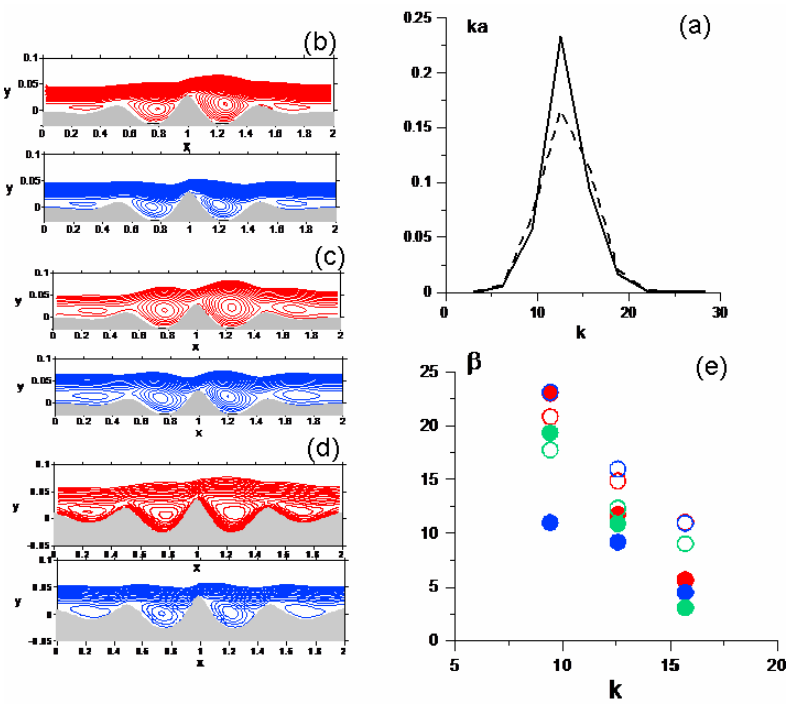

Fig.3. (a) The slope spectra of the wave-trains: solid line - *ka*=0.26, dashed line - *ka*=0.21.The stream line patterns of air flow of the air flow above the wave-train: (b) ka=0.21, c/u*=1.6, (c) ka=0.21, c/u*=3.2, (d) ka=0.26,c/u*=1.6. The red lines – DNS, the blue lines – the quasi-linear model. (e) The wind-wave interaction parameter for the individual harmonics of the wave-train: the red symbols - case (b), the blue symbols - case (c), the green symbols - case (d). The close symbols - DNS, the open symbols - the quasi-linear model.

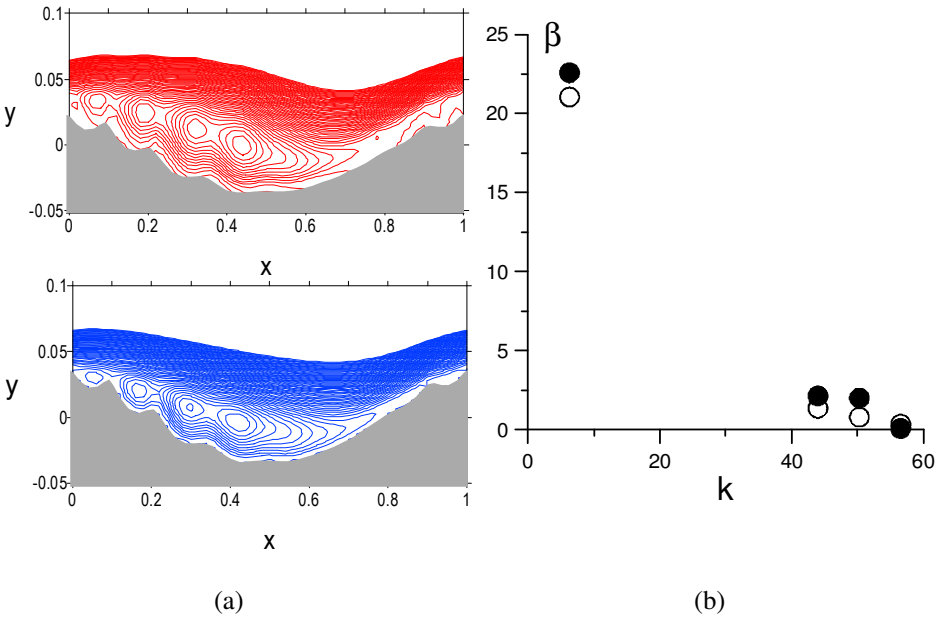

Fig.4. (a) The stream line patterns of air flow of the air flow above the steep surface wave with riding parasitic capillaries. The red lines – DNS, the blue lines – the quasi-linear model. (b) The wind-wave interaction parameter for the individual harmonics.

3.2.Wave trains and parasitic capillaries

It was found that quasi-linear approximation reproduces not only the air flow over the periodic quasi-harmonic wave, but also more complex above-the-surface shapes. We considered two cases of the wave forms typical for the waves in the ocean. First we performed DNS of the air turbulent boundary layer over two dimensional wavetrains. It was a purely model case, because we consider the simplest case of non-dispersive wave train with wide spectrum, where the spectral width is ¼ of the central frequency, and the integral slope is 0.21 and 0.26.

Comparison of the streamline patterns obtained within the DNS and quasi-linear models (Fig. 3, (b-d))shows, that even in case of this coherent wave-train the quasi-linear model gives close (not identical results) in comparison with DNS. We also calculated the wind-wave interaction parameter for the individual harmonics of the wave-train using Eq.(8) just as it is done in wave spectral models and compared it in Fig. 3 (e) with the prediction of the quasi-linear model. Obviously there is difference related to the coherent nonlinear effects which are neglected in the model. However, , the experimental error is below 50% for the central harmonic, which is usually below the measurement error in physical experiments.

Fig. 4 (a) compares the ensemble averaged stream-line patterns of the airflow over parasitic capillary waves riding on the crest of a steep wave. A two-dimensional surface wave with amplitude a, length λ, and phase velocity c, periodic in the x direction with slope $ka = 2\pi a/\lambda = 0.2$ is considered. Capillary ripples are modelled by the modulated high-frequency harmonic of the fundamental wave, which has the same phase velocity. The water surface is as follows:

$$\begin{aligned} x &= \xi - a_0 \sin k\xi - a_1\left(\sin k_1\xi + a_2\left[\sin\left(k_2\xi+\varphi\right)+\sin\left(k_3\xi-\varphi\right)\right]\right) \\ z &= a_0 \cos k\xi + a_1\left(\cos k_1\xi + a_2\left[\cos\left(k_2\xi+\varphi\right)+\cos\left(k_3\xi-\varphi\right)\right]\right) \end{aligned}, \tag{9}$$

where $k = 2\pi$ and a_0 are the wave number and amplitude of the fundamental wave, $k_1 = 8k$ and $a_1 = 0.05\,a_0$, are the wave number and amplitude of the ripples, $a_2 = 0.5$, $k_2 = 9k$, $k_3 = 7k$, $\varphi = -0.9$ are the parameters of the ripple modulation.

The stream-line patterns retrieved from DNS results and calculated within the quasi-linear model are not identical, but rather similar. Surprisingly the quasi-linear model reproduced the wind wave interaction parameter (see Fig. 4 (b)) even for capillaries. These results support the assumption, that the main nonlinear effect in wind-wave coupling is the deformation of the mean flow, well described by the quasi-linear model.

4. Applications of the quasi-linear approximation for processes in marine atmospheric boundary layer

In this section we discuss what the quasi-linear model can give for description of the aerodynamic resistance of the sea surface and growth rate of ocean wind waves. The wave field is parameterized by the growing sea spectrum in [28] with slightly modified Phillips' constant in accordance with [29]:

$$S\left(\vec{k}\right) = k^{-3}\left(B_l(k)+B_h(k)\right)\frac{2}{\pi}\cos^2\theta$$

$$B_l = \frac{0.006}{2}\Omega^{2/3}\begin{cases}\left(\dfrac{k}{k_p}\right)^{1/2}\exp\left\{-\dfrac{5}{4}\left(\dfrac{k}{k_p}\right)^2\left(1.7+6\log(\Omega)\right)^{\exp\left\{\frac{1}{2}\left(\frac{\sqrt{k}-\sqrt{k_p}}{0.08(1+4\Omega^{-3})\sqrt{k_p}}\right)^2\right\}}\right\} & k<k_0 \\ \left(\dfrac{k_0}{k_p}\right)^{1/2} & k>k_0\end{cases} \tag{10}$$

Here . $\Omega = \dfrac{U_{10}\omega_p}{g}$. is the wave age parameter, $\omega_p = \sqrt{gk_p}$, $k_0 = 9k_p$. $B_h(k)$ according to [30] is:

$$B_h = \frac{10^{-2}}{2}\left(1+3\ln\frac{u_*}{c}\right)\frac{u_*}{c}e^{-\frac{1}{4}\left(\frac{k}{k_m}-1\right)^2};k_m = \frac{2g}{\left(23cm/s\right)^2} \quad (11)$$

Comparison in Fig. 5 (a) shows that calculations within the quasi-linear model reproduce the surface drag coefficient within the experimental errors. The predicted wind wave growth rate is close to the data in [31, 32] (Fig. 6 (b)).

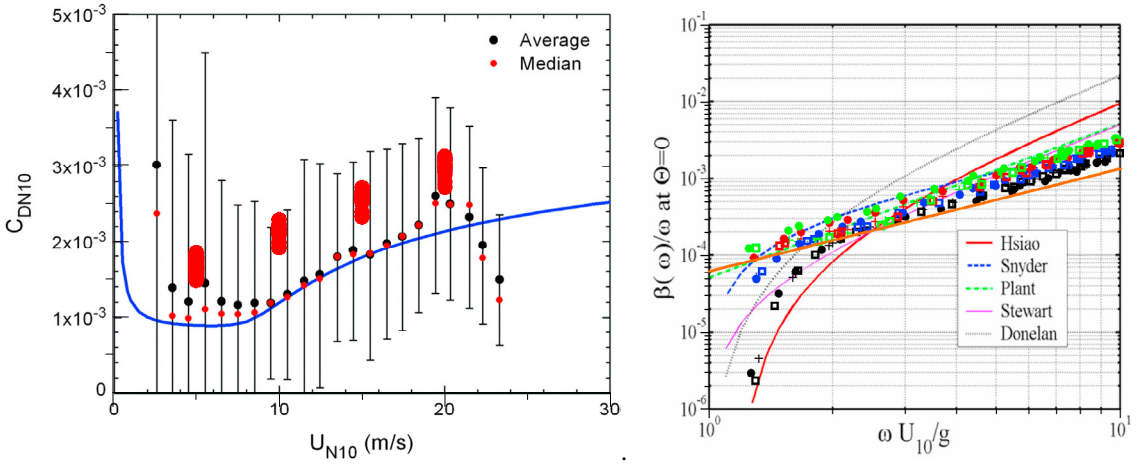

Fig.5. (a) Drag coefficient as a function of wind speed. Experimental data – from Andreas et al (2012). Red large symbols - calculations within the quasi-linear model. (b) Wind wave growth rate. Colored symbols - calculations within the quasi-linear model. Experimental data compilation adopted from Badulin, et al (2005).

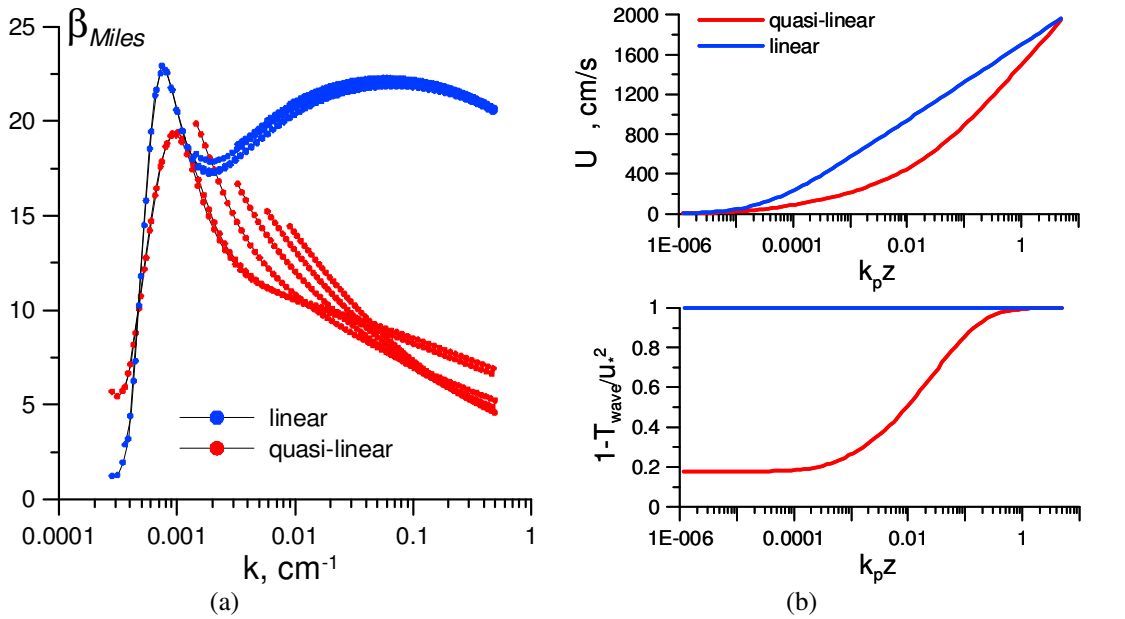

Fig.6. Growth rate of wind waves (a) and the wind velocity profile (top) and turbulent momentum flux (bottom) (b) calculated within the linear (blue lines) and quasi-linear (red) models. U_{10}=15 m/s.

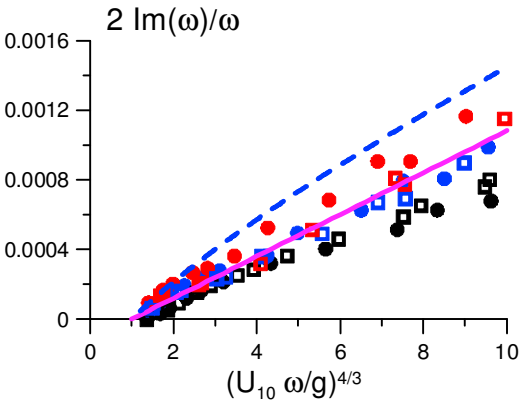

Fig.7. The growth rate of wind waves calculated within the quasi-linear model: black symbols U_{10}=5 m/s, blue symbols U_{10}=10 m/s, red symbols U_{10}=15 m/s. Different symbols corresponds to different models of the roughness height. The solid curve is fitting by Eq.(9), the dashed curve is the model by Hsiao, Shemdin (1983).

Note, that the wind-wave interaction parameter β calculated within the quasi-linear model is significantly reduced for short wave tail of the wind-wave spectra (compare the "linear" and "quasi-linear" β in Fig. 6 (a)). It can be explained by deformation of the wind velocity profile due to momentum flux from wind to waves (Fig. 6 (b)). As the result the shorter waves are interacting with the effectively decelerated air flow and their growth rate is reduced in comparison with the linear case.

Fig. 7 shows the relative growth rate as a function of dimensionless frequency $U_{10}\omega/g$ to degree 4/3, which can be well fitted by the linear function:

$$2\frac{\mathrm{Im}\,\omega}{\omega} = 0.00012\left(\left(\frac{U_{10}\omega}{g}\right)^{4/3} - 1\right) \tag{12}$$

Within the inertial interval of the surface wave spectra Eq.(9) provides the wind input term $S_{wind} \sim \omega^{7/3}\varepsilon(\omega)$ in the kinetic equation in agreement with [1].

5. Conclusions

In this paper we investigated applicability of a quasi-linear model for description turbulent boundary layer over steep surface waves. The model assumes that wave induced disturbances of the atmospheric turbulent boundary are described in linear approximation and the only nonlinear effect taken into account is momentum flux from wind to waves. The model was verified by special laboratory and numerical experiments. Experimental investigation of airflow over steep waves was performed by means of PIV technique. DNS of the airflow over waved surface was carried out for Re=15000. The best agreement is achieved for periodic waves, but for coherent wave trains and parasitic capillaries, the model also can reproduce the parameters of the wind turbulent flow over the waved water surface averaged over turbulent fluctuations and the wave growth rate. Basing on DNS an explanation of applicability of the quasi-linear model is suggested due to strong inhomogeneity of the separation zone in the transversal to wind direction. For the case of ocean waves with the continuous spectrum under the assumption of random phases of harmonics the quasi-linear model provides the growth rate of surface waves in the inertial interval of the surface wave spectrum proportional to $\omega^{7/3}$ in agreement with predictions in [1].

Acknowledgements

This work has been supported by the Russian Science Foundation (project 14-17-00667, 15-17-20009), Seventh Framework Programme (project PIRSES-GA-2013-612610) and Russian Foundation for Basic Research projects

(16-05-00839, 16-55-52022, 17-05-00703, 18-55-50005, 18-05-00265). Sergej Zilitinkevich additionally acknowledges support from the Academy of Finland project ABBA No. 280700, Alexander Kandaurov additionally acknowledges support by President grant for young scientists MC-2041.2017.5. The basic salary of the authors from IAP is financed by the government contract 0035-2014-0032. The experiments were performed at the Unique Scientific Facility "Complex of Large-Scale Geophysical Facilities" (http://www.ckp-rf.ru/usu/77738/).

References

1. V. Zakharov, D. Resio, A. Pushkarev, Balanced source terms for wave generation within the Hasselmann equation. *Nonlin. Processes Geophys.*, 2017, **24**: 581–597.
2. S. Badulin, A. V. Babanin, D. T. Resio, V. Zakharov, Weakly turbulent laws of wind-wave growth, *J. Fluid Mech*., 2007, **591:** 339–378.
3. A. Pushkarev, V. Zakharov, Limited fetch revisited: comparison of wind input terms, in surface wave modeling, *Ocean Model*., 2016, **103:** 18–37.
4. C. T. Hsu, E. Y. Hsu, On the structure of turbulent flow over a progressive water wave: theory and experiment in a transformed wave-following coordinate system. Part 2, *J. Fluid Mech*., 1983, **131**: 123–153.
5. C. T. Hsu, E. Y. Hsu, R. L. Street, On the structure of turbulent flow over a progressive water wave: theory and experiment in a transformed, wave-following co-ordinate system, *J. Fluid Mech.*, 1981, **105**: 87–117.
6. M. A. Donelan, A. V. Babanin, I. R. Young, M. L. Banner, McCormick C., Wave follower field measurements of the wind input spectral function. Part I: Measurements and calibrations, *J. Atmos. Oceanic Technol.*, 2005, **22(7)**: 799–813.
7. S. Kawai, Visualisation of air flow separation over wind wave crest under moderate wind, *Bound.-Layer Meteor.*, 2005, **21**: 93–104.
8. S. Kawai, Structure of air flow separation over wind wave crest, *Bound.-Layer Meteor.*, 1982, **23**: 503–521.
9. R. J. Adrian, Particle imaging techniques for experimental fluid mechanics, *Annu. Rev. Fluid Mech.*, 1991, **23**: 261–304.
10. N. Reul, H. Branger, J.-P. Giovanangeli, Air flow separation over unsteady breaking waves, *Phys. Fluids*, 1999, **11(7)**: 1959-1961.
11. N. Reul, H. Branger, J.-P. Giovanangeli, Air flow structure over short-gravity breaking water waves, *Bound.-Layer Meteor.*, 2008, **126**: 477–505.
12. F. Veron, G. Saxena, S. K. Misra, Measurements of the viscous tangential stress in the airflow above wind waves, *Geophys. Res. Lett.*, 2007, **34**: L19603.
13. Y. I. Troitskaya, D. A. Sergeev, O.S. Ermakova, G.N. Balandina, Statistical Parameters of the Air Turbulent Boundary Layer over Steep Water Waves Measured by the PIV Technique, *J. Phys. Oceanogr.*, 2011, **41**: 1421-1454.
14. M. P. Buckley, F. Veron, Structure of the airflow above surface waves, *J. Phys. Oceanogr.*, 2016, **46**: 1377–1397.
15. A. L. Fabrikant, Quasilinear theory of wind waves generation, *Izv. Atmos. Ocean. Phys.*, 1976, **12**: 858–862.
16. P. A. Janssen, Quasi-linear theory of wind wave generation applied to wave forecasting, *J. Phys. Oceanogr.*, 1991, **21**: 1631–1642.
17. J. W. Miles, On the generation of surface waves by shear flow. Part I, *J. Fluid Mech.,* 1957, **3**:185–204.
18. J. W. Miles, On the generation of surface waves by shear flows Part 3. Kelvin-Helmholtz instability, *J. Fluid Mech.*, 1959, **6(4)**: 583–598.
19. A. D. Jenkins, Quasi-linear eddy-viscosity model for the flux of energy and momentum to wind waves using conservation law equations in a curvilinear coordinate system, *J. Phys. Oceanogr.,* 1992, **22**: 843–858.
20. V. P. Reutov, Y. I. Troitskaya, On nonlinear effects due to water wave interaction with turbulent wind, *Izv. Russ. Acad. Sci., Atmos. Oceanic Phys.*, 1995, **31**: 825-834.
21. A. V. Smolyakov, Spectrum of the quadruple radiation of the plane turbulent boundary layer, *Acoust. Phys.,* 1973, **19(3)**: 420–425.
22. Y. I. Troitskaya, D. A. Sergeev, A. A. Kandaurov, G. A. Baidakov, M. A. Vdovin, and V. I. Kazakov, Laboratory and theoretical modeling of air-sea momentum transfer under severe wind conditions, *J. Geophys. Res.*, 2012, **117**: C00J21.
23. Y. I. Troitskaya, D. A. Sergeev, O.A. Druzhinin, A. A. Kandaurov, O.S. Ermakova, E.V. Ezhova, I. Esau, S. Zilitinkevich, Atmospheric boundary layer over steep surface waves, *Ocean Dyn.*, 2014, **64**: 1153–1161.
24. G. K. Batchelor, An introduction in fluid dynamics, *Cambridge University Press.,* 1967, 615.
25. O. A. Druzhinin, Y. I. Troitskaya, S. S. Zilitinkevich, Direct numerical simulation of a turbulent wind over a wavy water surface, *J. Geophys. Res., 2012,* **117**: C00J05.
26. P. Moin, J. Kim, The structure of the vorticity field in the turbulent channel flow. Part 1. Analysis of instantaneous fields and statistical correlations, *J. Fluid Mech.*, 1985, **155**: 441-464.
27. D. Yang, L. Shen, Direct-simulation-based study of turbulent flow over various waving boundaries, *J.Fluid Mech.*, 2010, **650**: 131-180
28. M. A. Donelan, W. J. Pierson, Radar Scattering and Equilibrium Ranges in Wind Generated Waves with Application to Scatterometry, *J. Geophys. Res.*, 1987, **92(5)**: 4971-5029.
29. D. T. Resio, C. E. Long, C. L. Vincent, Equilibrium-range constant in wind-generated wave spectra, *J. Geophys. Res.*, 109, 2004, **109**:C01018.
30. T. Elfouhaily, B. Chapron, K. Katsaros, D. Vandemark, A unified directional spectrum for long and short wind-driven waves, *J. Geophys. Res. Ocean.*, 1997, **102(7)**: 15781-15796.
31. S. V. Hsiao, O. H. Shemdin, Measurements of wind velocity and pressure with wave follower during Marsen, *J.Geophys.Res.*, 1983, **88**: 9841-9849.
32. R. L. Snyder, F. W. Dobson, J. A. Elliott, R. B. Long, Array measurement of atmospheric pressure fluctuations above surface gravity waves, *Journal of Fluid Mechanics,* 1981, **102**: 1-59.